

Carboxylic Acid- and Amine-Modified Pluronic F127-Based Thermoresponsive Nanogels as Smart Carriers for Brain Drug Delivery

Abegaz Tizazu Andrgie¹, Cheng-Han Liao², Tsung-Yun Wu^{2,3}, Hsueh-Hui Yang⁴, Horng-Jyh Harn^{5,6}, Shinn-Zong Lin^{5,7}, Yu-Shuan Chen^{4,5,8}, Hsieh-Chih Tsai^{2,3,9}

¹Department of Biotechnology, Debre Berhan University, Debre Berhan, Ethiopia; ²Graduate Institute of Applied Science and Technology, National Taiwan University of Science and Technology, Taipei, 106, Taiwan, Republic of China; ³Advanced Membrane Materials Center, National Taiwan University of Science and Technology, Taipei, 106, Taiwan; ⁴Department of Medical Research, Hualien Tzu Chi Hospital, Buddhist Tzu Chi Medical Foundation, Hualien, 970, Taiwan; ⁵Bioinnovation Center, Buddhist Tzu Chi Medical Foundation, Hualien, 970, Taiwan; ⁶Department of Pathology, Hualien Tzu Chi Hospital, Tzu Chi University, Buddhist Tzu Chi Medical Foundation, Hualien, 970, Taiwan; ⁷Department of Neurosurgery, Hualien Tzu Chi Hospital, Buddhist Tzu Chi Medical Foundation, Hualien, 970, Taiwan; ⁸Center for General Education, Tzu Chi University, Hualien, 970, Taiwan; ⁹R&D Center for Membrane Technology, Chung Yuan Christian University, Taoyuan, 320, Taiwan

Correspondence: Yu-Shuan Chen; Hsieh-Chih Tsai, Email yushuanchenxie@gmail.com; h.c.tsai@mail.ntust.edu.tw

Introduction: The blood-brain barrier (BBB) is a critical protective barrier that regulates the exchange of substances between the circulatory system and brain, restricting the access of drugs to brain tissues. Developing novel delivery strategies across the BBB is challenging but crucial. Multifunctional nanogels are promising drug carriers for delivering therapeutic agents to their intended target areas in the brain tissue.

Methods: This study introduced carboxylic acid- and amine-modified Pluronic F127 (ADF127 and EDF127)-based thermoresponsive nanogel systems as drug nanocarriers for brain tissues. The release profiles of 3-butylidenecephthalide (BP) from the nanogels were investigated in vitro in phosphate-buffered saline (pH 7.4) at 37 °C for 48 h. Additionally, the accumulation of DiR-labeled nanogels in vital organs was observed using fluorescence imaging.

Results: A relatively sustained BP release (27%) from ADF127, followed by rapid BP release (39%) from Pluronic F127 within the first 4 h were observed. In vivo studies using the C57BL/6JNarl mouse model showed that intravenously administered BP-loaded copolymeric nanogels exhibited a rapid BP distribution to the liver, spleen, heart, and kidney. DiR fluorescence intensity in the brain increased in the order Pluronic F127 < ADF127 < EDF127 copolymeric nanogels. Although the fluorescence intensity of DiR in the brain tissue was relatively lower than those in other vital organs, the DiR-labeled EDF127 copolymeric nanogels showed approximately 10-fold higher fluorescence intensity.

Conclusion: Positively charged drug carrier nanomaterials demonstrate a higher propensity for transfer through the BBB, significantly expanding the applicability of positively charged EDF127 nanogels as nanocarriers for in vivo brain tissue treatment and imaging. Therefore, owing to their increased permeability across the BBB, carboxylic acid- and amine-modified Pluronic F127 nanogels (EDF127 and ADF127) will also offer a promising approach for brain tissue treatment and imaging.

Keywords: blood-brain barrier, DiR labeling, permeability, sustained release, nanogels

Introduction

Numerous brain diseases have poor prognoses and low survival rates, with limited diagnostic and therapeutic options owing to the presence of the blood-brain barrier (BBB). The BBB regulates the exchange of substances between the circulatory system and brain, limiting the access of drugs to the brain parenchyma.¹⁻³ Surgical techniques are commonly used to overcome the limitations associated with the BBB and circumvent this natural biological barrier.⁴ However, these invasive approaches present a risks, including nerve damage and local inflammatory reactions. Recent research has focused on developing minimally invasive approach to deliver therapeutics through the BBB to brain tissues.^{5,6} Among



these, injectable thermosensitive hydrogels have gained attention as promising carriers owing to their unique properties of existing as free-flowing fluids at room temperature and converting into viscous gels at body temperature. Owing to their unique properties for minimally invasive administration, hydrogels in their liquid state can be administered anywhere behind biological barriers using a small needle, eliminating the need for invasive surgery.^{7–10} The In situ gel-forming materials form a depot for the sustained release of therapeutic agents.

In particular, in situ gel-forming thermosensitive nanogel systems have emerged as promising nanocarriers for therapeutic delivery. With advancements in nanotechnology, nanocarriers offer a promising solution owing to their small size, high surface-to-volume ratios, and tunable multifunctional properties, enabling injectable structures to penetrate physiological barriers.¹¹ The most interesting characteristics of nanocarriers as drug delivery systems are their high loading capacity, long-term stability, and responsiveness to different stimuli, leading to increased drug concentration in target tissues by prolonging drug diffusion time and increasing the possibility of drug penetration through physiological barriers.¹²

Thermoresponsive injectable nanogels composed of polymers can form gels in situ in response to various stimuli. Among the various thermoresponsive polymers, Pluronic F127 (PF 127) is a synthetic polymer that has been extensively investigated as an injectable nanogel for drug delivery applications.^{13–16} PF 127 is an amphiphilic triblock copolymer composed of hydrophilic poly(ethylene oxide) (PEO) and hydrophobic poly(propylene oxide) (PPO).¹⁷ Owing to its amphiphilic properties, PF127 can self-assemble into small micelle structures in aqueous solutions and undergo a sol-gel phase transition with increasing environmental temperature.¹⁸ At low temperatures, the PPO blocks exhibit weak hydrophobicity, and with increasing temperature, the PEO groups become dehydrated and aggregate to form micelles.^{8,19} The gelation temperature of PF127 can be controlled by adjusting the individual concentrations of the polymer blocks or by chemically modifying PF127 to increase its mechanical performance. This is because the native PF127 hydrogels exhibit low mechanical strength and stability despite their thermosensitive properties,²⁰ posing challenges in brain-targeting studies because the hydrogel might degrade too rapidly to effectively reach the brain. To address this issue, native and terminal-functionalized PF127 have been investigated for improved performance in brain-targeting applications. Modified PF127 polymers exhibit good mechanical properties as hydrogels and can encapsulate hydrophobic drugs in the hydrophobic core, providing stability and protection from external conditions.

In this study, the PF127 polymer was chemically modified using β -alanine (ADF127) and ethylenediamine (EDF127) for crosslinking the polymer chain through highly directed and intense hydrogen bonding interactions to improve the mechanical properties of the hydrogel. The intermolecular hydrogen bonding between the carboxyl and amine groups of β -alanine (ADF127) and ethylenediamine (EDF127) provides sufficient mechanical properties for the material to behave as a controlled drug carrier or to enable the sustained release of 3-butyridenepthalide (BP), an anticancer drug. The mechanical properties and thermo-response behavior of the copolymers were investigated using a rheometer in the dynamic oscillation mode, as reported in our previous work.²¹ Structural observations using scanning electron microscopy and the investigation of drug release and drug entrapment efficiency allowed the evaluation of the mechanical structure and stability of the modified nanogels. The in vivo biodistribution patterns of the DiR-loaded copolymeric hydrogels were investigated in a mouse model after intravenous injection using an in vivo imaging system (IVIS). This study further investigated the use of DiR-loaded EDF127 and ADF127 copolymeric nanogels to quantify and visualize their biodistribution in the brain tissue.

Materials and Methods

Synthesis of ADF127 and EDF127 Copolymers

ADF127 and EDF127 copolymers were synthesized using the procedure described by Wu et al.²¹ The hydroxyl group of PF127 (1.0 mmol) was activated using *N,N'*-disuccinimidyl carbonate (4.0 mmol) and 4-dimethylaminopyridine (4.0 mmol). The reactants were dissolved in 30 mL of anhydrous tetrahydrofuran and 5 mL of anhydrous dimethyl sulfoxide (DMSO) and reacted for 24 h at 25 °C. For ADF127, 4.0 mmol of β -alanine was dissolved in a small amount of ultrapure water. The intermediate was then added and stirred for 48 h at 25 °C. For EDF127, 4.0 mmol of ethylenediamine was mixed with the intermediate and stirred for 24 h at 25 °C. The solution was dialyzed for 5 days against

ultrapure water using a dialysis membrane with a molecular weight-cutoff of 1 kDa to remove any unreacted components. Subsequently, the products were freeze-dried for 3 days and then stored at 25 °C.

Characterization of ADF127 and EDF127 Copolymers

The ADF127 and EDF127 copolymers were characterized using ¹H-nuclear magnetic resonance (NMR) spectroscopy. ¹H NMR spectra of the two copolymers were recorded using a Bruker AVIII HD-600 instrument at 25 °C. The samples were prepared using DMSO-_{d6} as the solvent as described in detail in our previous study.²¹

Characterization of Micelle and Nanogel Morphology

The particle size distribution (PSD) of micelles was measured by performing dynamic light scattering (DLS) at a detection angle of 90°. Samples were prepared at a concentration of 10 mg/mL and dissolved in ultrapure water. The zeta potentials of copolymers PF127, ADF127, and EDF127 were measured using a Zeta-potential and Particle Size Analyzer (Horiba Zeta sizer-100 system, Malvern Instruments, UK). In addition, fluorescence-based assays were conducted using pyrene as the probe to determine the critical micelle concentration (CMC) of the thermosensitive copolymers. Initially, 0.1 M pyrene solution in acetone was diluted to 1.2×10^{-6} M using phosphate-buffered saline (PBS; 1×). Subsequently, the acetone was removed using a rotary evaporator. Copolymeric solutions with concentrations ranging from 2.5 to 8 mg/mL were mixed with pyrene in a 1:1 volume ratio. The samples were cooled at 4 °C for 2 h and stirred at 25 °C for 24 h. The CMC was evaluated using fluorescence spectroscopy (JASCO FP-8300, Japan). Field-emission scanning electron microscopy (FE-SEM; JEOL JSM-6500F, Japan) images were obtained to determine the pore structure and morphology of the polymeric nanogels and the nanogels encapsulated with anticancer drugs. The nanogels were initially heated from 25 to 37 °C, maintained in a water bath for 30 min, freeze-dried at -196 °C, and then quenched with liquid nitrogen.

Encapsulation of BP and Evaluation of in vitro Drug Release

BP (Sigma-Aldrich)-loaded PF127, ADF127, and EDF127 nanogels were synthesized using a simple mixing method. In a separate container, BP (1 g) was dissolved in 15 mL of 95% ethanol, and the resulting solution was slowly added to an 8% (w/v) copolymer solution with continuous stirring at 4 °C overnight to obtain a homogeneous solution. The mixture of the BP-copolymer solutions was then transferred to 37 °C and pH = 7.4 to mimic a body microenvironment. A dialysis membrane (MW = 1 kDa) was used to conduct the in vitro release analysis of the BP-encapsulated nanogels. An ultraviolet–visible (UV–Vis) spectrophotometer (JASCO V-730, Japan) was used to measure the BP intensity at 310 nm.

In vivo Body Distribution

C57BL/6JNarl mice were intravenously administered DiR-labeled hydrogels (n = 6) mice per copolymeric hydrogel). Untreated animals were used as controls (n = 3). All animal experiments were conducted in accordance with the recommendations of the Laboratory Animal Care and Use Committee of Hualien Tzu Chi Hospital, following the 3R principle (approval number: IACUC. 112–17). DiR was incorporated into the formulations at 8 wt% of the copolymer (PF127, ADF127, and EDF127). Mice were anesthetized and scanned 2 h after injection using a Lumina Series III IVIS (PerkinElmer, UK). Subsequently, the mice were euthanized, and their primary organs, including the heart, liver, spleen, lungs, kidneys, and brain, were harvested 2 h after injection. The collected organs were weighed and homogenized using a bead homogenizer. The tissue homogenate was then extracted three times with ethyl acetate to isolate BP. The chloroform phase was then evaporated and redissolved in acetonitrile and analyzed using liquid chromatography-mass spectrometry.

Statistical Analysis

All experiments were repeated at least thrice times. Data were presented as the mean ± standard deviation from a minimum of three independent experiments. Statistical significance was set at $P < 0.05$. One-way analysis of variance and linear regression were performed. Data analysis was conducted using the Origin software 2019b with 32-bit ink (OriginLab Corporation, USA).

Results and Discussion

Synthesis and Characterization of ADF127 and EDF127

PF127 was modified with carboxyl (ADF127) and amine (EDF127) terminal groups. The main signals from the repeated units of PF127 appeared at chemical shifts (δ) of 1.05 ppm (a, $-\text{CH}_3$ group of PPO), 3.30 ppm (d, $-\text{CH}$ group of PPO), 3.40 ppm (f, $-\text{CH}_2$ group of PPO), 3.45 ppm (i, $-\text{CH}_2$ group of PEO), and 3.50 and 4.05 ppm (h, $-\text{CH}_2$ group of PEO) (Figure 1). The electronegativity of oxygen influenced the chemical shift of the $-\text{CH}_2$ group at 4.05 ppm. In addition, the characteristic signal of the $-\text{NH}$ group at 7.20 ppm demonstrated the successful functionalization of the terminal active groups. Notably, the distinctive ADF127 peaks at 2.30 ppm (b) and 3.15 ppm (d) in Figure 1b represented the terminally active groups, whereas those of EDF127 were observed at 2.95 ppm (c).²¹

Particle Size of Micelles and Morphology of Nanogels

The size distribution of the BP-loaded copolymers (PF127, ADF127, and EDF127) was taken in triplicate, and the determined values are reported along with the polydispersity index (PDI). According to the results obtained from DLS, the PSD, the size distribution of the BP-loaded copolymers (PF127, ADF127, and EDF127), significantly increased at higher drug loads. This increase was primarily attributed to the encapsulation of hydrophobic drugs in the core of the copolymeric micelles. As the concentration of the encapsulated BP increased from 5 to 10 and 20 mg, the average particle size of BP-PF127 increased from 24 to 27 and 39 nm, respectively (Figure 2). Similarly, the average particle sizes of BP-ADF127 and EDF127 increased with increasing concentrations of encapsulated BP. In our previous study, we observed that the particle size of free EDF127 was higher than that of free PF127 and ADF127. Consequently, the drugs were readily incorporated into the EDF127 copolymeric micelles, resulting in average particle sizes of 22, 27, and 740 nm. When the concentration of encapsulated BP in the micelles was 5, 10, or 20 mg, the average particle sizes of the BP-ADF127 micelles were 22, 24, and 31 nm, respectively. The ADF127 copolymer formed stronger hydrogen bonds than PF127 and EDF127 in the micelle shells, which restricted free polymer integration during the self-assembly of the amphiphilic copolymer and the incorporation of drugs into the micelles, resulting in smaller micelle particles. The zeta potential values, along with the hydrodynamic size and polydispersity index (PDI), are summarized in Table 1. As expected from the chemical structure of the nanogels, the modified copolymers identified as ADF127 and EDF127 exhibited negative and positive zeta potential values, respectively (Figure 3).

CMC

CMC is a crucial factor in producing stable micelles for drug delivery, and it is essential to determine micelle stability under high-dilution conditions both *in vivo* and *in vitro*.²² Pyrene, a more sensitive fluorescent probe to hydrophobic environments, was used and encapsulated in the hydrophobic regions of copolymeric micellar aggregates.^{23,24} The intensity ratio of the first strong signal peak (I, 373 nm) to the second strong signal peak (I, 392.5 nm) (I373/I392.5) yielded the CMC value of PF127. Figure 4 shows the pyrene fluorescence emission spectra at various copolymer concentrations and the calculated CMC value of PF127 (CMC = 0.3108 mg/mL). The CMC values of ADF127 (CMC = 0.1304 mg/mL) and EDF127 (CMC = 0.1408 mg/mL)²¹ were relatively lower than that of PF127 (CMC = 0.41 mg/mL). This indicated that ADF127 and EDF127 were more stable than PF127 in the diluent. The presence of amide, amine, and carboxylic acid functional groups in the ADF127 and EDF127 copolymers enabled them to form stronger hydrogen bonds than F127, resulting in tighter integration of the polymer chain segments.

Morphology of Nanogels

The structure of freeze-dried copolymeric hydrogels, either unloaded or loaded with BP, were examined using SEM. Copolymeric hydrogels (PF-127, ADF127, and EDF127) have a porous structure, and the pore size varies with the hydrophilic and hydrophobic segment content. The pore size decreased when the hydrophobic drug was loaded into the hydrogels, indicating a physical interaction between the hydrophobic moieties of the polymer and drugs. Figure 5 shows the SEM images of the unloaded hydrogel and drug-loaded PF127, ADF127, and EDF127 copolymeric hydrogels. When the hydrogel encapsulated BP, the surface porosity decreased owing to the incorporation of the hydrophobic drug,

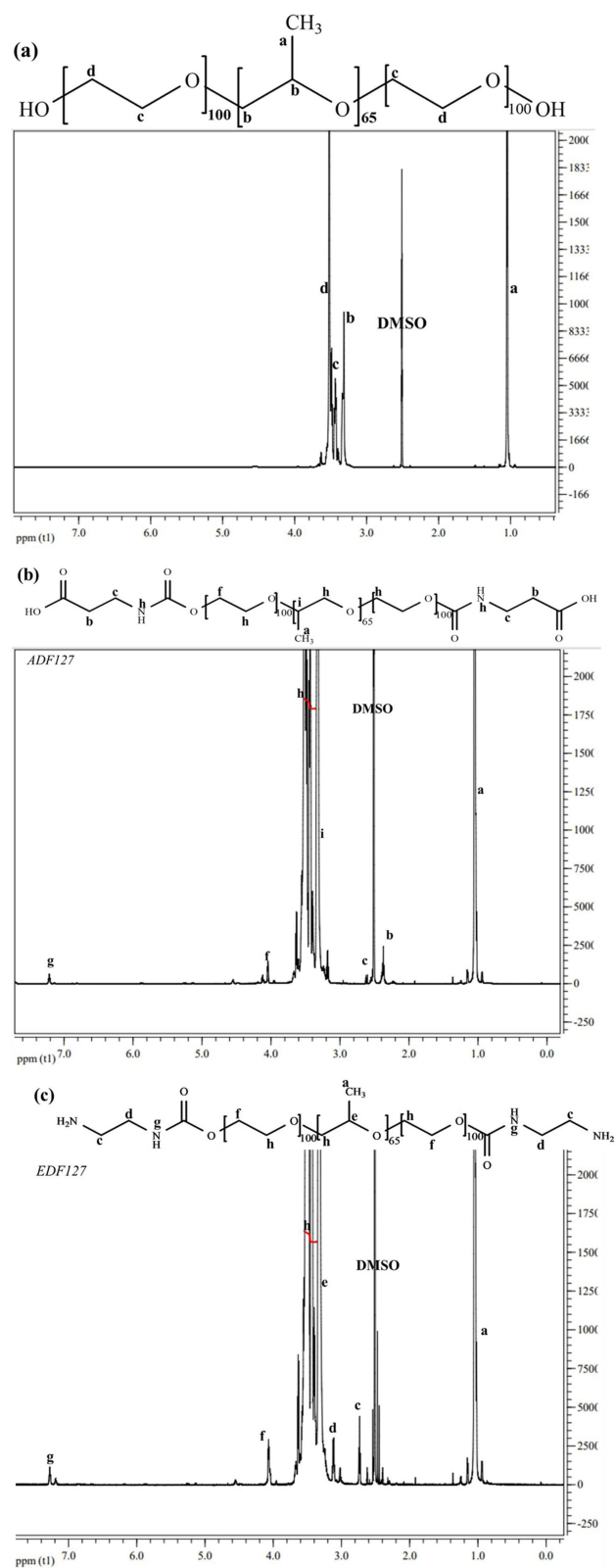


Figure 1 ¹H NMR spectra of (a) pluronic copolymer (b) β-alanine-modified pluronic copolymer (ADF127) and (c) ethylenediamine-modified pluronic copolymer (EDF127).

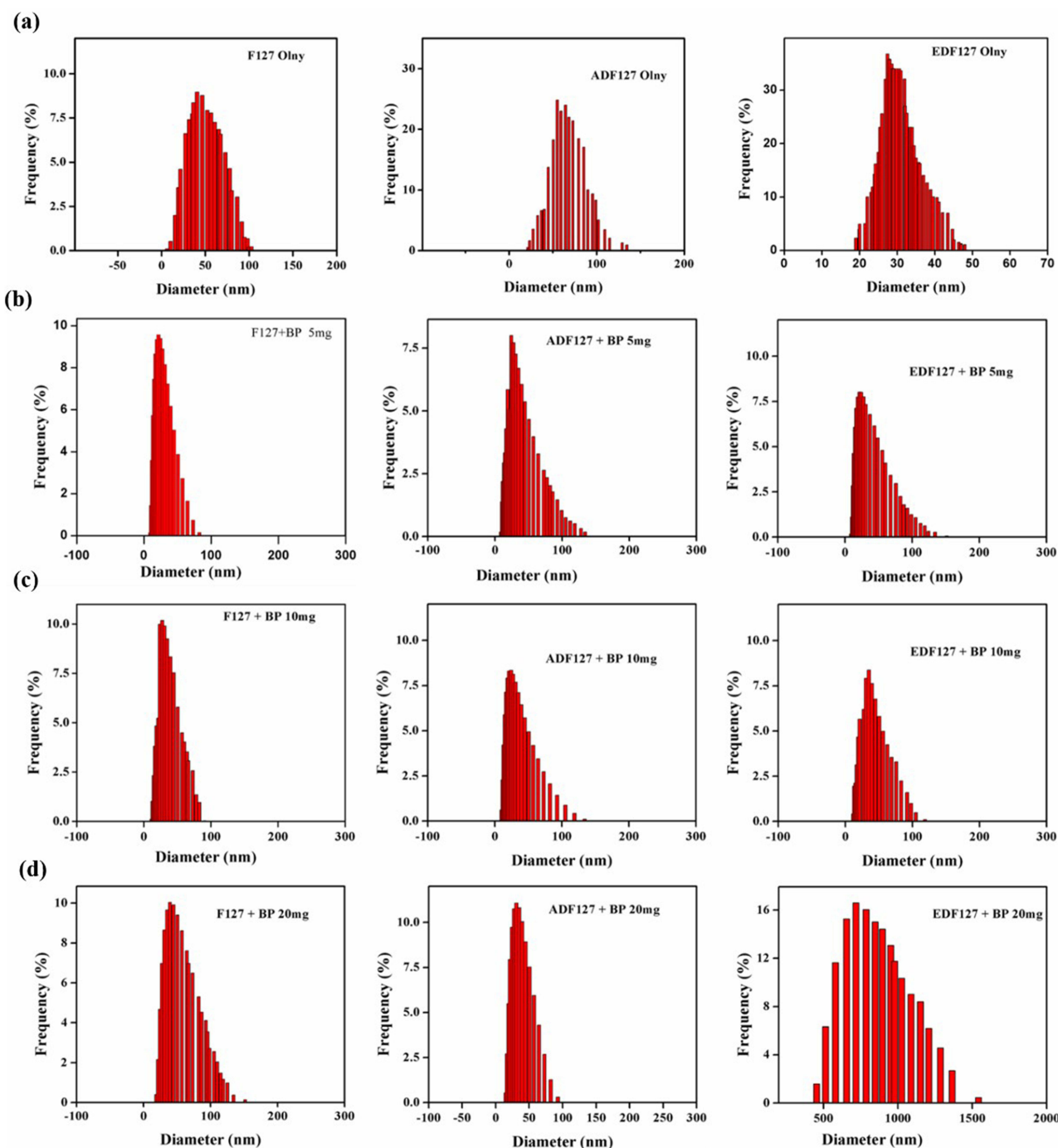


Figure 2 DLS profiles for the size distribution of (a) Polymers only, (b) Polymers + BP 5mg, (c) Polymers + BP 10mg, and (d) Polymers + BP 20mg. The concentration of each polymer is 10 mg/mL (1 wt%).

resulting in a reduction in mesh size. This decrease was observed when “BP, a hydrophobic drug, was encapsulated in the EDF127-BP polymeric hydrogel. This finding could explain the similarity in the particle size of the copolymer micelles and the weaker hydrogen bonds in the EDF127-BP micelles. This might contribute to the easy incorporation of the EDF127 polymer into micelles during self-assembly, resulting in increased network density and mesh size reduction. This result was consistent with the drug-release properties of the hydrogels. The large pore size of most hydrogels often leads to rapid drug release. As discussed for drug release, the PF127 and EDF127 copolymeric hydrogels with larger pores enabled the loading of more drugs into the gel matrix, subsequently leading to relatively rapid drug release.

Table 1 Hydrodynamic Size, Polydispersity Index, and ζ -Potential. PDI Is Polydispersity Index. The Results are Averages \pm standard Deviations (SD)

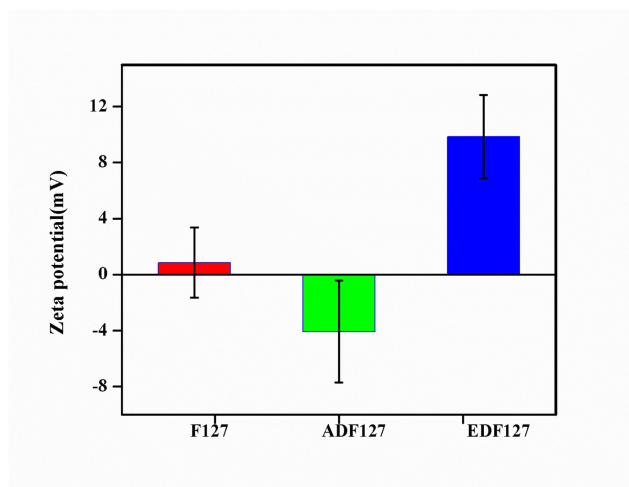
Micellar Hydrogels	Hydrodynamic Size(nm)	PDI	Zeta Potential [mV]
PF127	24	0.192	0.85 \pm 2.5
ADF127	22	0.168	-3.98 \pm 3.6
EDF127	21	0.187	9.87 \pm 2.9

In vitro drug release Analysis

The cumulative release of BP from the F127, ADF127, and EDF127 copolymeric hydrogels in vitro was measured using the dialysis membrane method in PBS (pH 7.4) at 37 °C for 48 h. The amount of released BP from the ADF-127 copolymeric nanogel was 27% in the first 4 h, whereas PF127 and EDF127 copolymer hydrogels increased the BP release to 38% and 26.5%, respectively (Figure 6). As observed in our previous studies, rheological tests of the ADF127 hydrogel and their interactions with hydrophobic drugs resulted in a slower initial burst release compared to EDF127 and PF127. A reduction in the burst release of ADF127 is desirable for the therapeutic action of the drug, enabling BP to maintain an optimal level for an extended therapeutic period. Following the burst release, the drug release rate decreased considerably owing to the stiffness of the copolymers, which exhibited sustained release from the nanogels because of hydrogen bonding with the copolymer terminal groups.

Incorporation of DiR into Nanogels

To determine the encapsulation efficacy of the copolymeric hydrogels and enable in vivo tracking after intravenous administration, we examined the incorporation of DiR, a near-infrared dye, into the copolymeric hydrogels. The UV-Vis absorption spectrum of the BP-loaded nanogels exhibited no absorption in the visible region (Figure S1). A strong absorption band centered at 778 nm was observed for DiR (Figures 7 and S2), which enabled whole-body imaging of the animals. We studied the incorporation of DiR into nanogels at different temperatures (-20, 4, and 37 °C). EDF127 showed DiR entrapment efficiency of 93.5% in the fresh micellar state and 82.25% and 81.01% at 4 and -20 °C storage conditions, respectively (Table 2). These results emphasized that the hydrogel pore sizes, composition of the copolymers, and hydrophobic characteristics of DiR influenced the encapsulation performance.²⁵ For EDF127, the copolymeric hydrogel has a larger pore size, contributing to its maximum swelling and DiR-loading capacity.

**Figure 3** Zeta potential of copolymeric micellar nanogels (F127, ADF127 and EDF127) with different coatings at pH 7.4.

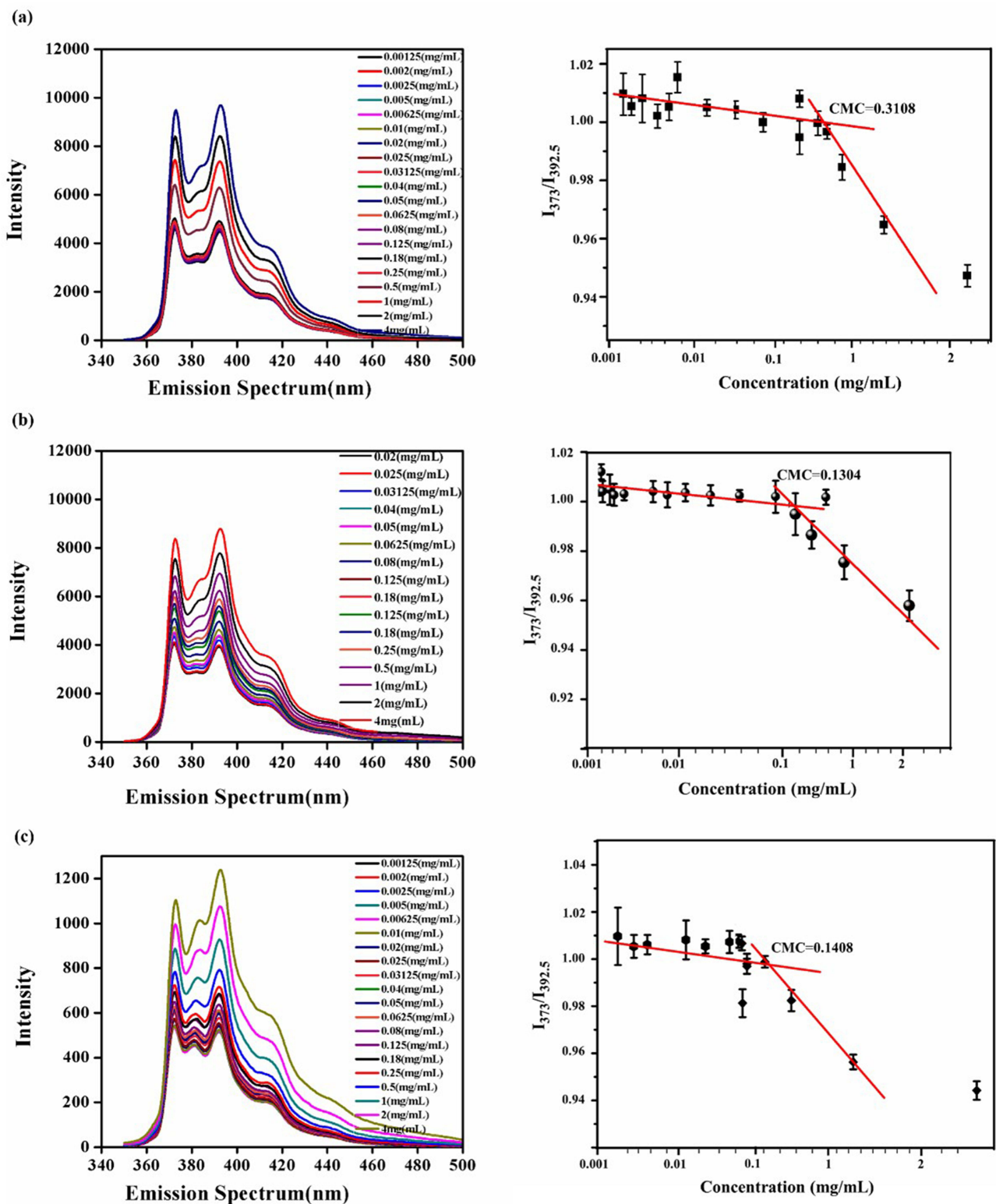


Figure 4 Pyrene fluorescence emission spectra in various copolymer concentrations and CMC of PF127 (a) ADF127 (b), and EDF127 (c). $I_{373}/I_{392.5}$ ratio from the emission spectrum versus concentration (mg/mL). Measurements are used to determine the CMC of the copolymers ($n = 3$).

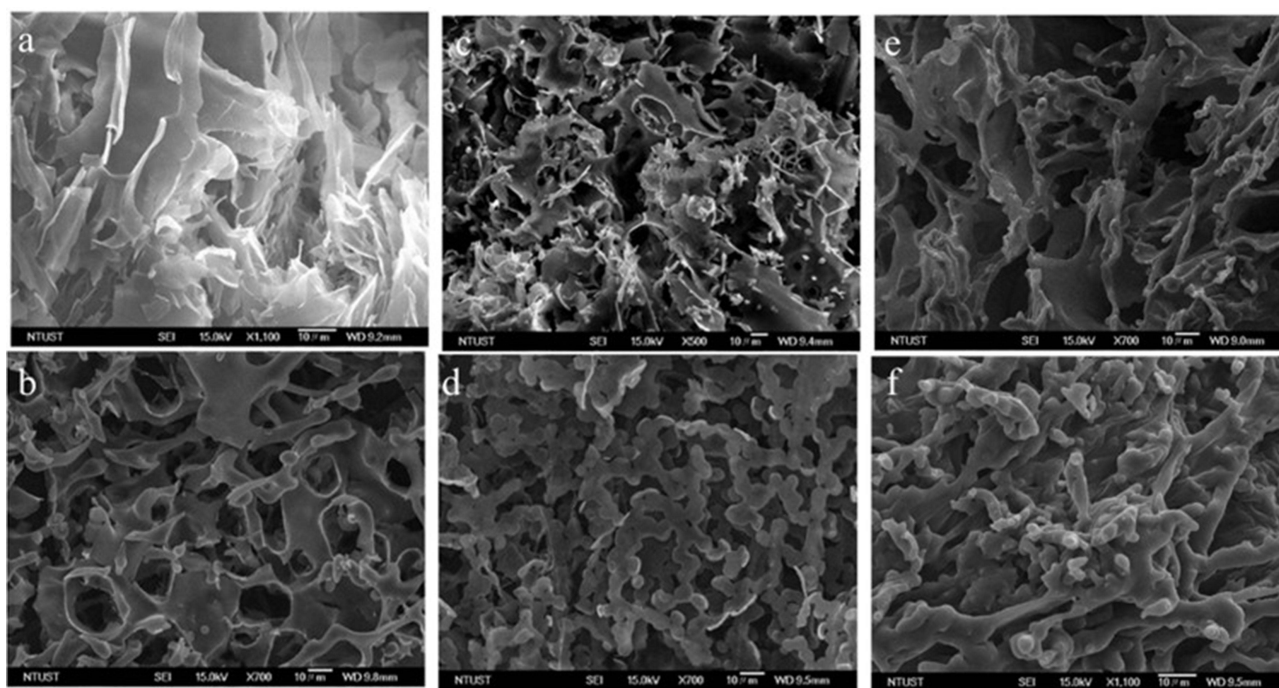


Figure 5 SEM images of (a) PF127 only, (b) BP- PF127, (c) ADF127 only, (d) BP-ADF127, (e) EDF127 only, and (f) BP-EDF127 at 37 °C.

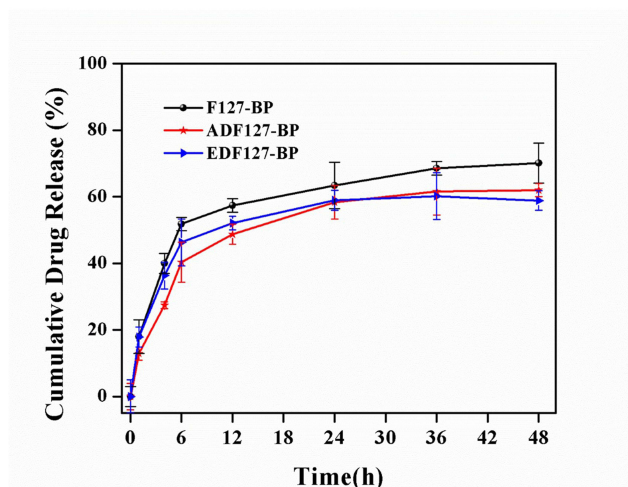


Figure 6 In vitro cumulative drug-release kinetics of BP-loaded PF127, ADF127, and EDF127 in phosphate-buffered saline (1x).

In vivo Biodistribution

To investigate the in vivo distribution patterns of DiR after intravenous administration, copolymeric hydrogel formulations of F127, ADF127, and EDF127 were used as carriers of DiR. For all three copolymeric hydrogels, radioactive signals were enhanced in whole-body imaging and significantly increased compared to the control (Figure 8a and b). After 2 h of post-injection of DiR-loaded hydrogels, the mice were euthanized, and their organs were harvested for ex vivo imaging and BP quantification. Compared to EDF127-loading BP and ADF127-loading BP, F127-loading BP was preferentially distributed in the liver and spleen, while its distribution in the heart, kidneys, and lungs was roughly equivalent to those of ADF127 and EDF127 (Figure 8c and d). In most cases, nanomaterials with a typical size range of 10–50 nm exhibited high accumulation in the liver and spleen but were prone to elimination by the kidneys.²⁶ Although

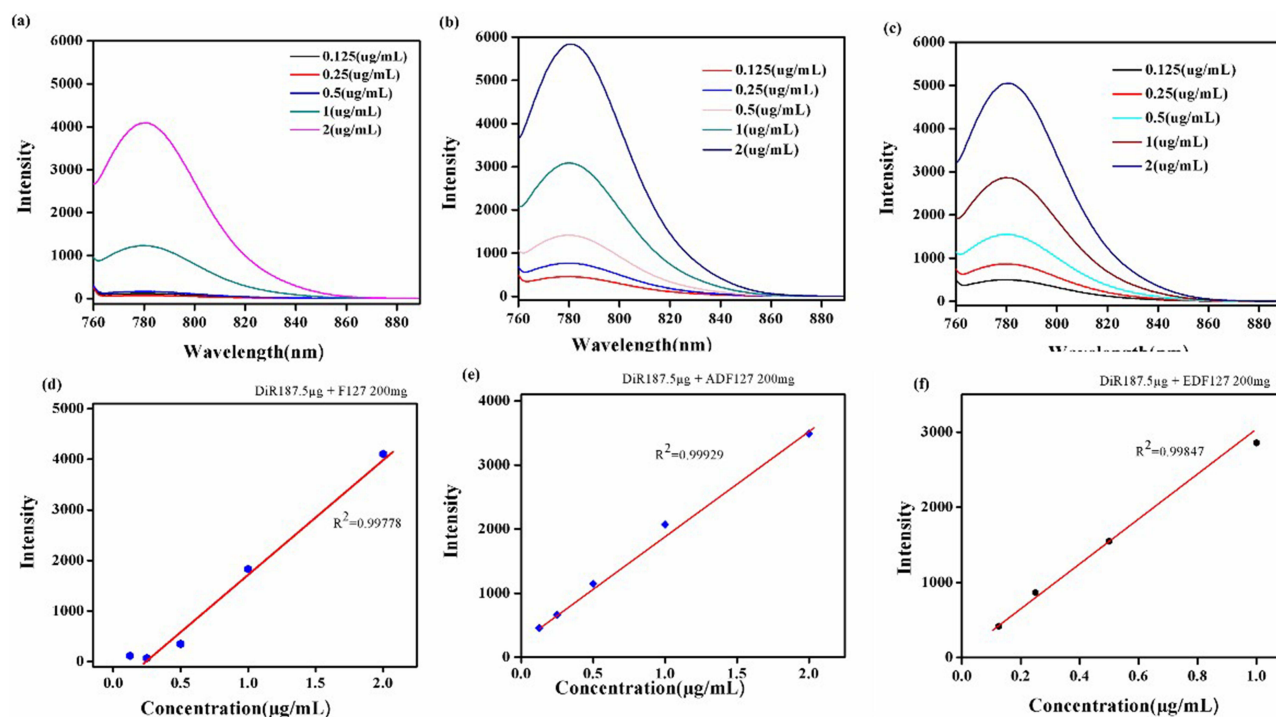


Figure 7 Normalized concentration-dependent fluorescence spectra of (a) PF127, (c) ADF127, and (e) EDF127. Intensity of PL spectra versus sample concentration of DiR-loaded nanogel (b, d, and f).

the size of nanomaterials is a critical factor for BBB penetration, an optimal size range, particularly between 50 and 100 nm, has been reported to facilitate BBB penetration without encountering renal elimination.^{27,28}

The accumulation of DiR in the brain was relatively lower than that in other vital organs. However, the fluorescence intensity of DiR in the brain tissue of EDF127 mice was approximately 10-fold higher than those of F127 and ADF127 mice. EDF127 contains a positively charged functional group at the PF127 terminal (Figure 8e and f). A major challenge in drug delivery to brain tissue is the BBB, which impedes the successful delivery and accumulation of therapeutic molecules.^{5,29,30} Development of a drug delivery system that successfully crosses the BBB is a promising strategy for transporting therapeutics to the brain. Endothelial cells of the BBB possess a more negative charge owing to a higher quantity of proteoglycans.³¹ This finding suggested that positively charged drug carrier materials were more likely to be transferred through the BBB.^{20,32} Positively charged EDF127 was more likely to cross the BBB than negatively charged ADF127, which might lead to greater accumulation of DiR in the brain tissue. Therefore, ensuring effective BBB penetration and targeted delivery was crucial for developing future drug delivery systems aimed at the brain tissue.

Although PF127, ADF127, and EDF127 containing BP or DiR can be delivered to the brain, their distribution patterns differ between these two agents. This difference might be attributed to the variations in the molecular weights of BP (approximately 188.22) and DiR (1013.41). Notably, BP distribution in the liver was significantly lower when delivered via EDF127 than when delivered via PF127, which could be one reason for the higher DiR distribution observed when delivered via EDF127.

Table 2 DiR Entrapment Efficiency of PF127, ADF127, and EDF127 Copolymer Nanogels at Different Storage Conditions

Micellar Hydrogels	Fresh Micelle (37 °C)	Micelle (4 °C)	Micelle (-20 °C)
PF127	80.12%	73.69%	82.23%
ADF127	82.81%	58.34%	58.34%
EDF127	93.65%	82.23%	85.01%

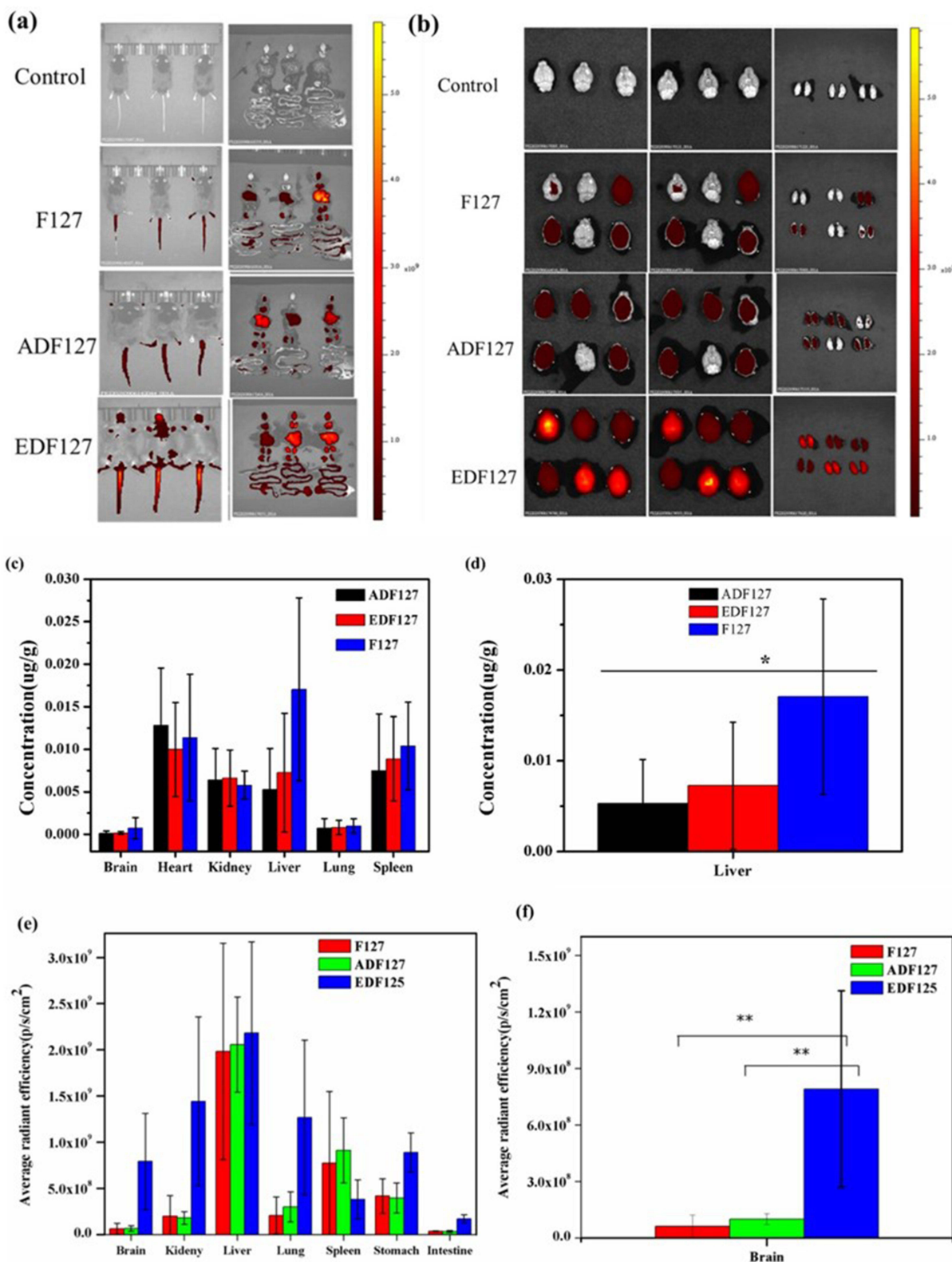


Figure 8 In vivo biodistribution 2 hours after drug administration: In vivo imaging of **(a)** whole body (left) and whole organ (right); and **(b)** dorsal- (left), ventral- (middle), and split-brain (right) sections of SKH2 mice In vivo imaging of the whole body (left) and whole organs (right) with DiR-loaded PF127, ADF127, and EDF17 nanogels. **(c)** and **(d)** Biodistribution of BP in the brain, heart, kidney, liver, lung, and spleen 2 h post-injection, **(e)** and **(f)** Ex vivo average radiant efficiency of DiR-nano gels with their biodistribution in the brain, kidney, liver, lung, spleen, and intestine tissues: * $p < 0.05$, ** $p < 0.01$.

Conclusion

In this study, EDF127 and ADF127 thermoresponsive nanogels were successfully designed as smart carriers for brain drug delivery by introducing carboxyl and amine functional groups into PF127 as chain extenders to enhance mechanical stability of the nanogels. The in vitro drug release from the ADF127 and EDF127 nanogels was prolonged (65%; 48 h), demonstrating sustained release and prolonged retention time of the drug in nanogels. The release of anticancer drug BP from ADF-127 copolymeric nanogel was 27% in the first 4 h, effectively reducing the initial burst release and maintaining optimal BP levels for an extended therapeutic period. An animal study was conducted to evaluate the in vivo biodistribution of BP-loaded nanogels using intravenous administration, which resulted in rapid distribution of BP to the liver, spleen, heart, and kidney. For in vivo studies using DiR-labeled nanogels, efficient accumulation of DiR in vital organs was observed using fluorescence imaging. Although the fluorescence intensity of DiR in the brain tissue was lower than that in other vital organs, the accumulation of DiR in the brain tissues increased in the order PF127 < ADF127 < EDF127 copolymeric nanogels. Positively charged drug carrier nanomaterials are more likely to pass through the BBB. Therefore, positively charged EDF127 copolymeric nanogels have considerable potential for application in drug delivery systems for brain tissue treatment and imaging.

Abbreviations

BBB, blood-brain barrier; BP, 3-butyridenephthalide; PEO, poly(ethylene oxide); PPO, poly(propylene oxide); DMSO, dimethyl sulfoxide; NMR, nuclear magnetic resonance; PBS, phosphate-buffer saline, CMC, critical micelle concentration; DLS, dynamic light scattering; FE-SEM, Field-emission scanning electron microscopy, UV-Vis, ultraviolet-visible.

Acknowledgments

The authors gratefully acknowledge the financial support from National Science and Technology Council (Taiwan) 113-2221-E-303-001, 112-2221-E-303-002 and NSTC-111-2622-E-303-001.

Disclosure

The authors report no conflicts of interest in this work.

References

1. Pardridge WM. Drug transport across the blood-brain barrier. *J Cereb Blood Flow Metab.* 2012;32(11):1959–1972. doi:10.1038/jcbfm.2012.126
2. Zhang S, Gan L, Cao F, et al. The barrier and interface mechanisms of the brain barrier, and brain drug delivery. *Brain Res Bull.* 2022;190:69–83. doi:10.1016/j.brainresbull.2022.09.017
3. Wu D, Chen Q, Chen X, et al. The blood–brain barrier: structure, regulation, and drug delivery. *Signal Trans Targeted Ther.* 2023;8(1):217. doi:10.1038/s41392-023-01481-w
4. Narsinh KH, Perez E, Haddad AF, et al. Strategies to improve drug delivery across the blood–brain barrier for glioblastoma. *Curr Neurol Neurosci Rep.* 2024;24(5):123–139. doi:10.1007/s11910-024-01338-x
5. Ding S, Khan AI, Cai X, et al. Overcoming blood–brain barrier transport: advances in nanoparticle-based drug delivery strategies. *Mater Today.* 2020;37:112–125. doi:10.1016/j.mattod.2020.02.001
6. Finbloom JA, Sousa F, Stevens MM, et al. Engineering the drug carrier biointerface to overcome biological barriers to drug delivery. *Adv Drug Delivery Rev.* 2020;167:89–108. doi:10.1016/j.addr.2020.06.007
7. Bellotti E, Schilling AL, Little SR, et al. Injectable thermoresponsive hydrogels as drug delivery system for the treatment of central nervous system disorders: a review. *J Control Release.* 2021;329:16–35. doi:10.1016/j.jconrel.2020.11.049
8. Chen -Y-Y, Wu H-C, Sun J-S, et al. Injectable and thermoresponsive self-assembled nanocomposite hydrogel for long-term anticancer drug delivery. *Langmuir.* 2013;29(11):3721–3729. doi:10.1021/la400268p
9. Parameswaran-Thankam A, Parnell CM, Watanabe F, et al. Guar-based injectable thermoresponsive hydrogel as a scaffold for bone cell growth and controlled drug delivery. *ACS omega.* 2018;3(11):15158–15167. doi:10.1021/acsomega.8b01765
10. Karimi M, Sahandi Zangabad P, Ghasemi A, et al. Temperature-responsive smart nanocarriers for delivery of therapeutic agents: applications and recent advances. *ACS Appl Mater Interfaces.* 2016;8(33):21107–21133. doi:10.1021/acsmi.6b00371
11. Cuggino JC, Blanco ERO, Gugliotta LM, et al. Crossing biological barriers with nanogels to improve drug delivery performance. *J Control Release.* 2019;307:221–246. doi:10.1016/j.jconrel.2019.06.005
12. Dong X. Current strategies for brain drug delivery. *Theranostics.* 2018;8(6):1481–1493. doi:10.7150/thno.21254
13. Chatterjee S, Hui PC-L, Wat E, et al. Drug delivery system of dual-responsive PF127 hydrogel with polysaccharide-based nano-conjugate for textile-based transdermal therapy. *Carbohydr Polym.* 2020;236:116074. doi:10.1016/j.carbpol.2020.116074
14. PJ RJ, Oluwafemi OS, Thomas S, et al. Recent advances in drug delivery nanocarriers incorporated in temperature-sensitive Pluronic F-127–A critical review. *J Drug Delivery Sci Technol.* 2022;72:103390. doi:10.1016/j.jddst.2022.103390

15. Salama AH. PLURONIC F127 and ITS applications. *Pharmacologyonline*. 2021;2:1393–1403.
16. Sharun K, Banu SA, Mamachan M, et al. Thermoresponsive and injectable pluronic F127 hydrogel for loading adipose-derived mesenchymal stem cells. *Discov Med*. 2024;36(181):294–307. doi:10.24976/Discov.Med.202436181.28
17. Alexandridis P, Hatton TA. Poly (ethylene oxide) poly (propylene oxide) poly (ethylene oxide) block copolymer surfactants in aqueous solutions and at interfaces: thermodynamics, structure, dynamics, and modeling. *Colloids Surf A*. 1995;96(1–2):1–46. doi:10.1016/0927-7757(94)03028-X
18. Xie R, López-Barrón CR, Greene DG, et al. Comicellization of binary PEO–PPO–PEO triblock copolymer mixtures in ethylammonium nitrate. *Macromolecules*. 2018;51(4):1453–1461. doi:10.1021/acs.macromol.7b02115
19. Bercea M, Darie RN, Niță LE, et al. Temperature responsive gels based on pluronic F127 and poly (vinyl alcohol). *Ind Eng Chem Res*. 2011;50(7):4199–4206. doi:10.1021/ie1024408
20. Asimakidou E, Tan JKS, Zeng J, et al. Blood-brain barrier-targeting nanoparticles: biomaterial properties and biomedical applications in translational neuroscience. *Pharmaceutics*. 2024;17(5):612. doi:10.3390/ph17050612
21. Wu T-Y, Huang -C-C, Tsai H-C, et al. Mucin-mediated mucosal retention via end-terminal modified Pluronic F127-based hydrogel to increase drug accumulation in the lungs. *Biomater Adv*. 2024;156:213722. doi:10.1016/j.bioadv.2023.213722
22. Lu Y, Zhang E, Yang J, et al. Strategies to improve micelle stability for drug delivery. *Nano Res*. 2018;11(10):4985–4998. doi:10.1007/s12274-018-2152-3
23. Hutchinson JA, Hamley IW, Torras J, et al. Self-assembly of lipopeptides containing short peptide fragments derived from the gastrointestinal hormone ppy 3–36: from micelles to amyloid fibrils. *J Phys Chem A*. 2019;123(3):614–621. doi:10.1021/acs.jpcc.8b11097
24. Afzal M, Ghosh S, Das S, et al. Endogenous activation-induced delivery of a bioactive photosensitizer from a micellar carrier to natural DNA. *J Phys Chem A*. 2016;120(44):11492–11501. doi:10.1021/acs.jpcc.6b08283
25. Hu X. A review of recent advances in drug loading, mathematical modeling and applications of hydrogel drug delivery systems. *J Mater Sci*. 2024;1–40.
26. Zha S, Liu H, Li H, et al. Functionalized nanomaterials capable of crossing the blood–brain barrier. *ACS nano*. 2024;18(3):1820–1845. doi:10.1021/acsnano.3c10674
27. Hersh AM, Alomari S, Tyler BM. Crossing the blood-brain barrier: advances in nanoparticle technology for drug delivery in neuro-oncology. *Int J mol Sci*. 2022;23(8):4153.
28. Shilo M, Sharon A, Baranes K, et al. The effect of nanoparticle size on the probability to cross the blood-brain barrier: an in-vitro endothelial cell model. *J Nanobiotechnology*. 2015;13:19. doi:10.1186/s12951-015-0075-7
29. Daneman R, Prat A. The blood-brain barrier. *Cold Spring Harb Perspect Biol*. 2015;7(1):a020412. doi:10.1101/cshperspect.a020412
30. Omid Y, Kianinejad N, Kwon Y, et al. Drug delivery and targeting to brain tumors: considerations for crossing the blood-brain barrier. *Expert Rev Clin Pharmacol*. 2021;14(3):357–381. doi:10.1080/17512433.2021.1887729
31. Walter FR, Santa-Maria AR, Mészáros M, et al. Surface charge, glycocalyx, and blood-brain barrier function. *Tissue Barriers*. 2021;9(3):1904773. doi:10.1080/21688370.2021.1904773
32. Miao Y-B, Zhao W, Renchi G, et al. Customizing delivery nano-vehicles for precise brain tumor therapy. *J Nanobiotechnol*. 2023;21(1):32. doi:10.1186/s12951-023-01775-9

International Journal of Nanomedicine

Publish your work in this journal

The International Journal of Nanomedicine is an international, peer-reviewed journal focusing on the application of nanotechnology in diagnostics, therapeutics, and drug delivery systems throughout the biomedical field. This journal is indexed on PubMed Central, MedLine, CAS, SciSearch®, Current Contents®/Clinical Medicine, Journal Citation Reports/Science Edition, EMBase, Scopus and the Elsevier Bibliographic databases. The manuscript management system is completely online and includes a very quick and fair peer-review system, which is all easy to use. Visit <http://www.dovepress.com/testimonials.php> to read real quotes from published authors.

Submit your manuscript here: <https://www.dovepress.com/international-journal-of-nanomedicine-journal>

Dovepress
Taylor & Francis Group